Accepted Manuscript

Protective Effects of Topical Vitamin C Compound Mixtures Against Ozone-Induced Damage In Human Skin

Giuseppe Valacchi, PhD, Alessandra Pecorelli, PhD PharmD, Giuseppe Belmonte, MS, Erika Pambianchi, Franco Cervellati, PhD, Stephen Lynch, PhD, Yevgeniy Krol, Christian Oresajo, PhD

PII: S0022-202X(17)30184-7

DOI: 10.1016/j.jid.2017.01.034

Reference: JID 742

To appear in: *The Journal of Investigative Dermatology*

Received Date: 8 November 2016

Revised Date: 18 January 2017

Accepted Date: 31 January 2017

Please cite this article as: Valacchi G, Pecorelli A, Belmonte G, Pambianchi E, Cervellati F, Lynch S, Krol Y, Oresajo C, Protective Effects of Topical Vitamin C Compound Mixtures Against Ozone-Induced Damage In Human Skin, *The Journal of Investigative Dermatology* (2017), doi: 10.1016/j.jid.2017.01.034.

PROTECTIVE EFFECTS OF TOPICAL VITAMIN C COMPOUND MIXTURES AGAINST OZONE-INDUCED DAMAGE IN HUMAN SKIN

Giuseppe Valacchi PhD[1-2*], Alessandra Pecorelli PhD PharmD[1-3], Giuseppe Belmonte MS[1], Erika Pambianchi[1], Franco Cervellati PhD[1], Stephen Lynch PhD[4], Yevgeniy Krol[5], Christian Oresajo PhD[4]

[1]Plants for Human Health Institute, Department of Animal Sciences, NC State University, NC Research Campus, 600 Laureate Way, Kannapolis, NC 28081; [2]Department of Life Sciences and Biotechnology, University of Ferrara, Via L. Borsari, 44121 Ferrara, Italy; [3]Child Neuropsychiatry Unit, University Hospital, AOUS, Viale M. Bracci, 53100 Siena, Italy; [4]L'Oréal Research and Innovation, Clark, NJ, USA; [5]SkinCeuticals Inc., New York, NY, USA.

*Corresponding Author

Prof. Giuseppe Valacchi
Dept. of Animal Science
NC State University,
Plants for Human Health Institute
NC Research Center
28081 – Kannapolis (NC) USA

Short title: ozone induced skin damage is prevented by vitamin C

Environmental pollution is a challenge to modern society, especially in developing countries. It has been estimated that more than 90% of the urban population live with pollutant levels in excess of WHO standard limits. (www.WHO.int).

There are numerous studies supporting the noxious effect that O_3 exposure can have on cutaneous tissues; however, a drawback in the research has been a lack of data derived from humans. Recently, a retrospective study from Xu et al., collecting data from almost 70,000 patients, was able to correlate the rising incidence of ER visits for urticaria, eczema, and contact dermatitis to an increased ambient level of O_3 (Xu et al., 2011). The evidence cited in current literature suggests the need to further investigate the harmful effect of O_3 on human skin, as well as to evaluate possible measures to counteract its effect. For this reason, the objective of the present study was to investigate whether O_3 exposure, at a level that has been observed in polluted cities (0.8ppm), could affect skin tissue responses, and whether vitamin C compound mixtures can prevent O_3 induced skin damage.

An 8-day study was conducted on 15 subjects after obtaining written informed consent. Institutional Review Board approval was obtained (Allendale Institutional Review Board; 7015-090-104/106-002; August 10, 2015). The subjects' forearms were randomized and divided into 4 zones: (1) MIX1 (15% L-ascorbic acid, 1% Alpha-tocopherol, 0.5% Ferulic acid, "CE Ferulic", SkinCeuticals Inc., NY), (2) MIX2 (10% L-ascorbic acid, 2% Phloretin, 0.5% Ferulic acid; "Phloretin CF", SkinCeuticals Inc., NY), (3) untreated/O_3 exposed, (4) untreated/unexposed on the lateral forearm. The subjects' forearms were exposed to 0.8 ppm O_3 for 3 hrs/day for 5 consecutive days and 1 punch biopsy (3 mm) from the 4 different areas was collected. Subjects were monitored for adverse events throughout the course of the study.

It is generally demonstrated that although O_3 is not a radical species per se, its toxic effects are mediated through free radical reactions leading to lipid peroxidation (Pryor, 1994).

Known byproducts of lipid peroxidation are the α-β unsaturated aldehyde 4-hydroxynonenal (4HNE) and the 8-iso $PGF_{2\alpha}$, isoprostane (Poli et al., 2008). As shown in Fig.1, after O_3 exposure, there was a significant increase of both 4HNE protein adducts (2.4-fold) and 8-iso $PGF_{2\alpha}$ levels (2.1-fold) (green signal) in human skin compared to the control tissues, while treatment with MIX1 and MIX2 significantly prevented this effect (Fig. S1-S2). This data supports previous work, where a clear increase of 4HNE levels was observed in skin of O_3-exposed SKH-1 mice as a consequence of O_3 reaction with the outmost skin surface lipids (Valacchi et al., 2002).

Oxidative stress stimuli can cause activation of "redox sensitive transcription factors"; such as *nuclear factor kappa B* (NF-κB). Its activation involves the dissociation of the cytosolic NF-κB/IκB complex, allowing NF-κB to translocate into the nucleus and binds to DNA for the transcription for growth factors and pro-inflammatory cytokines (Siomek, 2012). As shown in Fig.1, when the skin tissues were exposed to O_3, there was an evident increase in p65 signal (green fluorescence) of *circa* 2.4-fold. The tissues treated with both MIX1 and MIX2 clearly showed a decrease in NF-κB expression (Fig. S3). The ability of O_3 to induce NF-κB activation in keratinocytes was previously demonstrated in *in vitro* and animal models (Valacchi et al., 2004, 2016), and we suggest that its activation is a trigger for a series of biological events leading to inflammation (Ali et al., 2016). As an example, in psoriatic epidermis, inflammatory cytokines induce a constitutive activation of NF-κB, which promotes keratinocyte hyper-proliferation (Yan et al., 2015).

Considering the activation of NF-κB is related to increased oxidative stress, being able to quench the oxidative damage induced by O_3 could prevent its activation. Indeed, O_3 exposure is able to deplete antioxidant levels in the skin (Thiele et al., 1997; Valacchi et al., 2000), and their topical application can prevent O_3-induced skin damage and NF-κB activation. This data was further confirmed by the upregulation of cyclooxygenase-2 (COX-2), a well-known inflammatory

marker regulated by NF-κB (Korbecki et al., 2013). As shown in Fig.1, O_3 induced an increase (2.7-fold) of COX-2 levels compared to unexposed skin. The treatment with MIX1 and MIX2 significantly prevented (circa 70%) the increased expression of COX-2 induced by O_3 (Fig.S4). An increased COX-2 level subsequent to NF-κB activation was observed in previous studies on skin from O_3-exposed SKH-1 mice (Valacchi et al., 2004). Preventing the induction of COX-2 through the use of vitamin C compound mixtures (MIX1 and MIX2) can have significant benefits for skin health.

Oxidative stress and inflammation, the two pathways activated by O_3, can compromise the integrity of skin by promoting connective tissue degradation via MMPs expression, and O_3 has been shown to modulate the activities of enzymes involved in connective tissue turnover, such as MMP-9 (Fortino et al., 2007). In our study, MMP-9 (active form) levels were significantly increased after O_3 exposure (Fig.1), nearly 2-fold, (red signal). Of note, the treatment with MIX1 and MIX2 significantly prevented this effect. While MMP-9 activity was altered by O_3, TIMP-1, the endogenous inhibitor of metalloproteinases, was not affected. (Fig.S5-S6).

Given the important function of the collagen fibers in the maintenance of skin elasticity and resilience, collagen I and III were assessed. As shown in Fig.1, after O_3 exposure there was a significant decrease in both types of skin collagens (green signal) compared to control (-64% and -60%, respectively). Pre-treatment with MIX 1 and MIX2 significantly prevented collagen marker loss. We suspect the lower detection of collagen is mainly due to the oxidation of the proteins rather than to its degradation (Fig.S7-S8). Interestingly, the observed effect of O_3 on collagen and MMPs levels provides evidence that O_3 exposure could also affect wound healing processes, as previously shown in animal models (Lim et al., 2008).

The oxidative effect of O_3 on human skin (depletion of vitamin E and oxidized lipids increase), was previously described by He et al. (2006) via tape stripping. To our knowledge, the

current study with biopsy analysis, is the first conducted in humans able to show that O_3 exposure can broadly affect cutaneous tissue. Topical application of vitamin C compound mixtures appears capable of preventing the observed effects.

Conflict of Interest

The authors state no conflict of interest.

References

Ali F, Khan BA, Sultana S. Wedelolactone mitigates UVB induced oxidative stress, inflammation and early tumor promotion events in murine skin: plausible role of NFkB pathway. Eur J Pharmacol. 2016;786:253-64.

Fortino V, Maioli E, Torricelli C, Davis P, Valacchi G. Cutaneous MMPs are differently modulated by environmental stressors in old and young mice. Toxicol Lett. 2007;173:73-9.

He QC, Tavakkol A, Wietecha K, Begum-Gafur R, Ansari SA, Polefka T. Effects of environmentally realistic levels of ozone on stratum corneum function. Int J Cosmet Sci. 2006;28:349-57.

Korbecki J, Baranowska-Bosiacka I, Gutowska I, Chlubek D. The effect of reactive oxygen species on the synthesis of prostanoids from arachidonic acid. J Physiol Pharmacol. 2013;64:409-21.

Lim Y, Phung AD, Corbacho AM, Aung HH, Maioli E, Reznick AZ, et al. Modulation of cutaneous wound healing by ozone: differences between young and aged mice. Toxicol Lett. 2006 Jan 5;160(2):127-34.

Poli G, Schaur RJ, Siems WG, Leonarduzzi G. 4-hydroxynonenal: a membrane lipid oxidation product of medicinal interest. Med Res Rev. 2008;28:569-631.

Pryor WA. Mechanisms of radical formation from reactions of ozone with target molecules in the lung. Free Radic Biol Med. 1994;17:451-65.

Siomek A. NF-κB signaling pathway and free radical impact. Acta Biochim Pol. 2012;59:323-31.

Thiele JJ, Traber MG, Tsang K, Cross CE, Packer L. In vivo exposure to ozone depletes vitamins C and E and induces lipid peroxidation in epidermal layers of murine skin. Free Radic Biol Med. 1997;23:385-91.

Valacchi G, Weber SU, Luu C, Cross CE, Packer L. Ozone potentiates vitamin E depletion by ultraviolet radiation in the murine stratum corneum. FEBS Lett. 2000;466:165-8.

Valacchi G, van der Vliet A, Schock BC, Okamoto T, Obermuller-Jevic U, Cross CE, et al. Ozone exposure activates oxidative stress responses in murine skin. Toxicology. 2002;179:163-70.

Valacchi G, Pagnin E, Corbacho AM, Olano E, Davis PA, Packer L, et al. In vivo ozone exposure induces antioxidant/stress-related responses in murine lung and skin. Free Radic Biol Med. 2004;36:673-81.

Valacchi G, Muresan XM, Sticozzi C, Belmonte G, Pecorelli A, Cervellati F, et al. Ozone-induced damage in 3D-Skin Model is prevented by topical vitamin C and vitamin E compound mixtures application. J Dermatol Sci. 2016;82:209-12.

Xu F, Yan S, Wu M, Li F, Xu X, Song W, et al. Ambient ozone pollution as a risk factor for skin disorders. Br J Dermatol. 2011;165:224-5.

Yan S, Xu Z, Lou F, Zhang L, Ke F, Bai J, et al. NF-κB-induced microRNA-31 promotes epidermal hyperplasia by repressing protein phosphatase 6 in psoriasis. Nat Commun. 2015;6:7652-66.

FIGURE LEGEND

Figure 1. Exposure to unhealthy levels of ground-level ozone (0.8 ppm) damages the human cutaneous tissue. Representative immunofluorescence images of human skin tissues (n=15) stained with antibodies for: (**a**) 4hydroxynonenal (4HNE), (**b**) 8-iso Prostaglandin F_2 alpha (IsoP), (**c**) NF-κB p65 subunit (NFκB), (**d**) cyclooxygenase-2 (COX2), (**e**) active form of metalloproteinase 9 (MMP9), (**f**) tissue inhibitor of metalloproteinase-1 (TIMP-1), (**g**) type I collagen (COL I) and (**h**) type I collagen (COL III). Original magnification x630. (**i**) Immunofluorescent signal (green or red fluorescence) was semi-quantified by using ImageJ software. Results are presented as means ± standard deviation. $*P < 0.05$ *vs* Air.

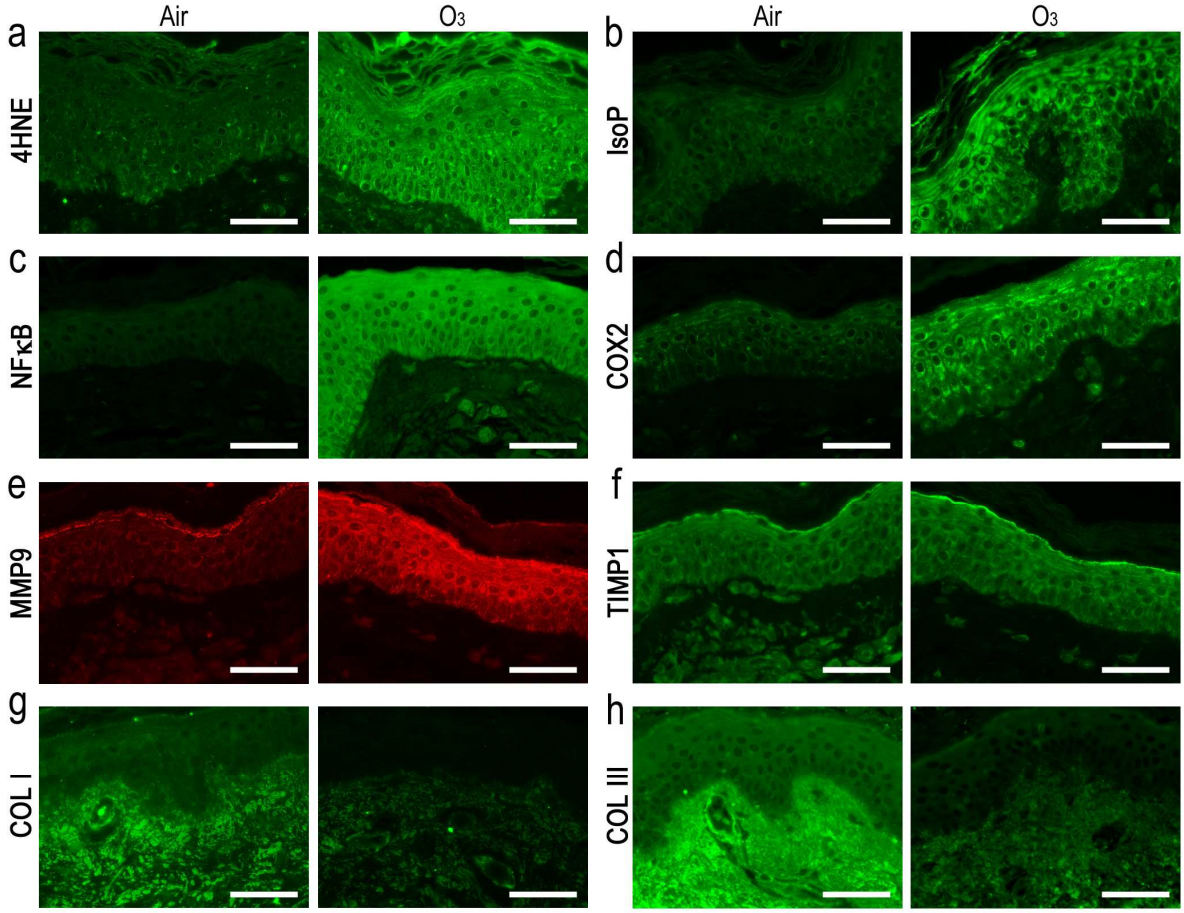
Air
O3
a
4HNE
b
IsoP
c
NFκB
d
COX2
e
MMP9
f
TIMP1
g
COL I
h
COL III

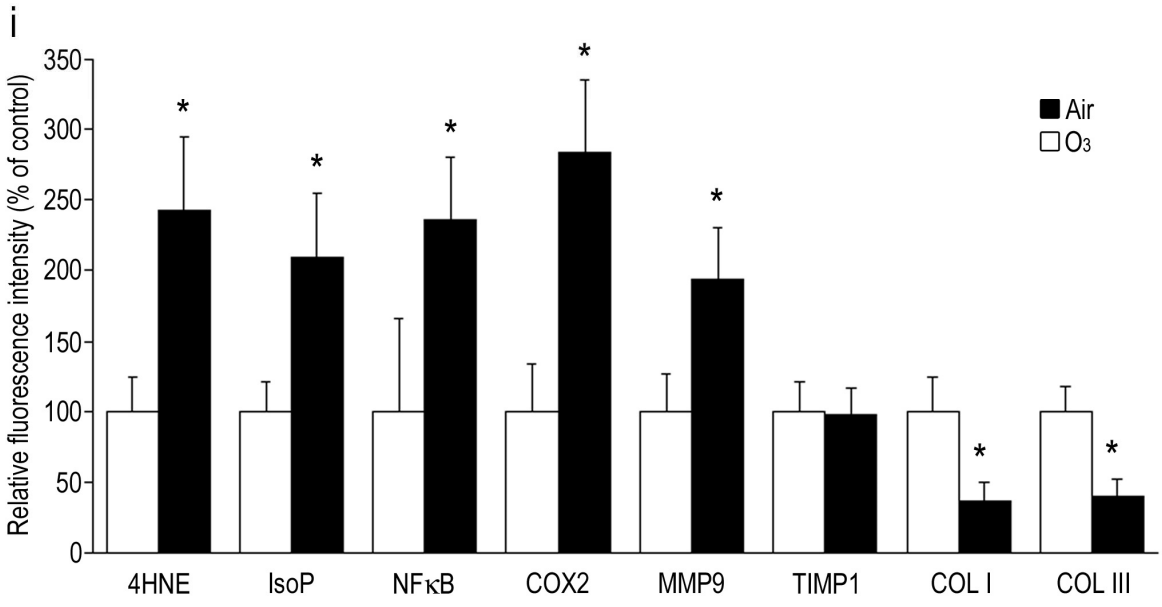
i
Relative fluorescence intensity (% of control)
350
300
250
200
150
100
50
0
Air
O3
*
4HNE
IsoP
NFκB
COX2
MMP9
TIMP1
COL I
COL III

MATERIALS AND METHODS

Subject enrollment

A total of 15 volunteer subjects were enrolled in the study. The Caucasian subjects, aged 18–55 years, were inclusive of both men and women. Each participant gave written consent before enrollment into the study. Institutional Review Board approval was obtained (Allendale Institutional Review Board; 7015-090-104/106-002; August 10, 2015).

All subjects were free of any systemic or dermatological disorders, including a known history of allergies or other medical conditions that could interfere with the conduct of the study or interpretation of results. They agreed to use no topical products or cosmetics on their forearms other than those comprising the clinical protocol. The subjects were also instructed to avoid excessive sun exposure and artificial tanning, as well as swimming, for the duration of the study.

At the pre-treatment visit, subjects were screened, and those who met all inclusion and exclusion criteria were enrolled in the study.

Experimental research protocol

The subjects' forearms were randomized (right and left) and were divided into 4 zones: (1) MIX 1 (15% L-ascorbic acid + 1% Alpha-tocopherol + 0.5% Ferulic acid; CE Ferulic, SkinCeuticals Inc., New York, NY), (2) MIX 2 (10% L-ascorbic acid + 2% Phloretin + 0.5% Ferulic acid; Phloretin CF, SkinCeuticals Inc., New York, NY), (3) untreated/ O_3 exposed (Fig.1), (4) untreated/unexposed on the lateral forearm The product-treated zones were treated daily for 3 days (day 1 – day 3) prior to O_3 exposure, and throughout the course of the study (day 4 – day 8). The subjects' forearms were exposed to 0.8 ppm O_3 for 3 hrs/day for 5 consecutive days (Fig.2).

Ozone exposure

O_3 was generated from O_2 by an electrical corona arc discharge (Model 306 ozone Calibration Source, 2B Technologies, Ozone Solution, USA), as previously described (Valacchi et al., 2016). Briefly, the O_2–O_3 mixture (95% O_2, 5% O_3) was combined with ambient air and allowed to flow into a Teflon-lined exposure chamber. The O_3 concentration in the chamber was adjusted to varying ppm outputs and continuously monitored by an O_3 detector. The forearms were

exposed inside a plexiglass box, in direct exposure to O_3. Temperature and humidity were monitored during exposures (25°C and 45–55%, respectively).

The following pictures show the apparatus and procedure for forearm exposure to O_3 (Fig. 1); as it is possible to observe in Fig. 2, three zones were selected in the randomized forearm of subject, each of 2 cm^2: (1) MIX 1 (15% L-ascorbic acid + 1% Alpha-tocopherol + 0.5% Ferulic acid; CE Ferulic, (2) MIX 2 (10% L-ascorbic acid + 2% Phloretin + 0.5% Ferulic acid; Phloretin CF, (3) untreated/ O_3 exposed zone.

Fig. 1. Zones selected in the randomized forearm for O_3 exposure. Areas 1, 2 and 3 were randomly chosen for the different treatments.

Fig. 2. The Ozone Exposure Chamber. The ozone generator, settled up to 0.8 ppm, was connected to a Plexiglass exposure chamber in a chemical hood.

Human tissue collection

A total of four 3-mm punch biopsies were collected from each subject immediately after the last O_3 exposure (day 8). Three biopsies were collected from the O_3-exposed lateral forearm; one each from the following zones: CE Ferulic treated, Phloretin CF treated, no product treated. One biopsy was collected from untreated lateral forearm. Total number of biopsies: four biopsies per subject (60 biopsies total).
Samples were fixed in 10% buffered Formalin Solution for immunohistochemical analysis.

Immunofluorescence

The fixed punch biopsies were embedded in paraffin and used to obtain 3 μm thick tissue sections. Sections were briefly deparaffinised in xylene and rehydrated in graded ethanol solutions (100%, 95%, 80%, and 70%), 5 minutes each, and washed in dH_2O. Antigen retrieval was obtained by incubation with 10 mM sodium citrate buffer (pH 6.0) at a sub-boiling temperature for 20 min. Sections were then cooled for 10 min, washed in phosphate-buffered saline (PBS), and incubated overnight at 4?C with the following antibodies: 4-hydroxynonenal (Merck Millipore, Milano, Italy), 8-iso Prostaglandin F_2 alpha (Abcam, Milan, Italy), NF-κB p65 subunit (Santa Cruz Biotechnology, Inc., Heidelberg, Germany), cyclooxygenase-2 (Cell Signaling Technology, Danvers, MA, USA), metalloproteinase-9 (Thermo Fisher Scientific Inc., Monza, Italy), Type I collagen (Abcam, Cambridge, UK) and Type III collagen (Thermo Fisher Scientific Inc., Monza, Italy). The slides were washed 3 times with PBS and incubated with the fluorochrome-conjugated secondary antibodies: Alexa Fluor 488 or 568 (Thermo Fisher Scientific Inc.) for 1 hour at room temperature in the dark. Slides were washed with PBS and mounted with Antifade. In each case, a negative control was generated by omitting the primary antibody. Images were acquired with a microscope Leica AF CTR6500HS (Microsystems).

Immunofluorescence quantification

Fluorescent signal was semi-quantified by using ImageJ software, using the corrected total section fluorescence (CTSF) formula, according to a previously reported method (Potapova et al., 2011; McCloy et al., 2014). An area of interest (ROI) in each section was selected using the polygon drawing/selection tool, in order to analyze only the fluorescence signal from the skin tissue. Selecting the ‘Measure' function from the “Analyze” menu provided the area, the mean grey value,

and the integrated density of the ROI. The mean background level was obtained by measuring the intensity of regions untreated with primary-Ab (expressing a basic fluorescence noise of the analyzed tissue, i.e. the background). We used the following formula to calculate the CTSF: Integrated Density of ROI - (Area of ROI X Fluorescence of background readings).
CTSF values were examined in a total of 180 section (3 per condition/marker)

Statistical analysis

All subjects who completed the study were included in the statistical analysis. Results are expressed as means ± SD. Statistical comparisons were performed using the Student t-tests. A p value of < 0.05 was considered statistically significant.

Reference

Potapova TA, Sivakumar S, Flynn JN, Li R, Gorbsky GJ. Mitotic progression becomes irreversible in prometaphase and collapses when Wee1 and Cdc25 are inhibited. Mol Biol Cell. 2011;22(8):1191-206.

McCloy RA, Rogers S, Caldon CE, Lorca T, Castro A, Burgess A. Partial inhibition of Cdk1 in G 2 phase overrides the SAC and decouples mitotic events. Cell Cycle. 2014;13(9):1400-12. doi: 10.4161/cc.28401.

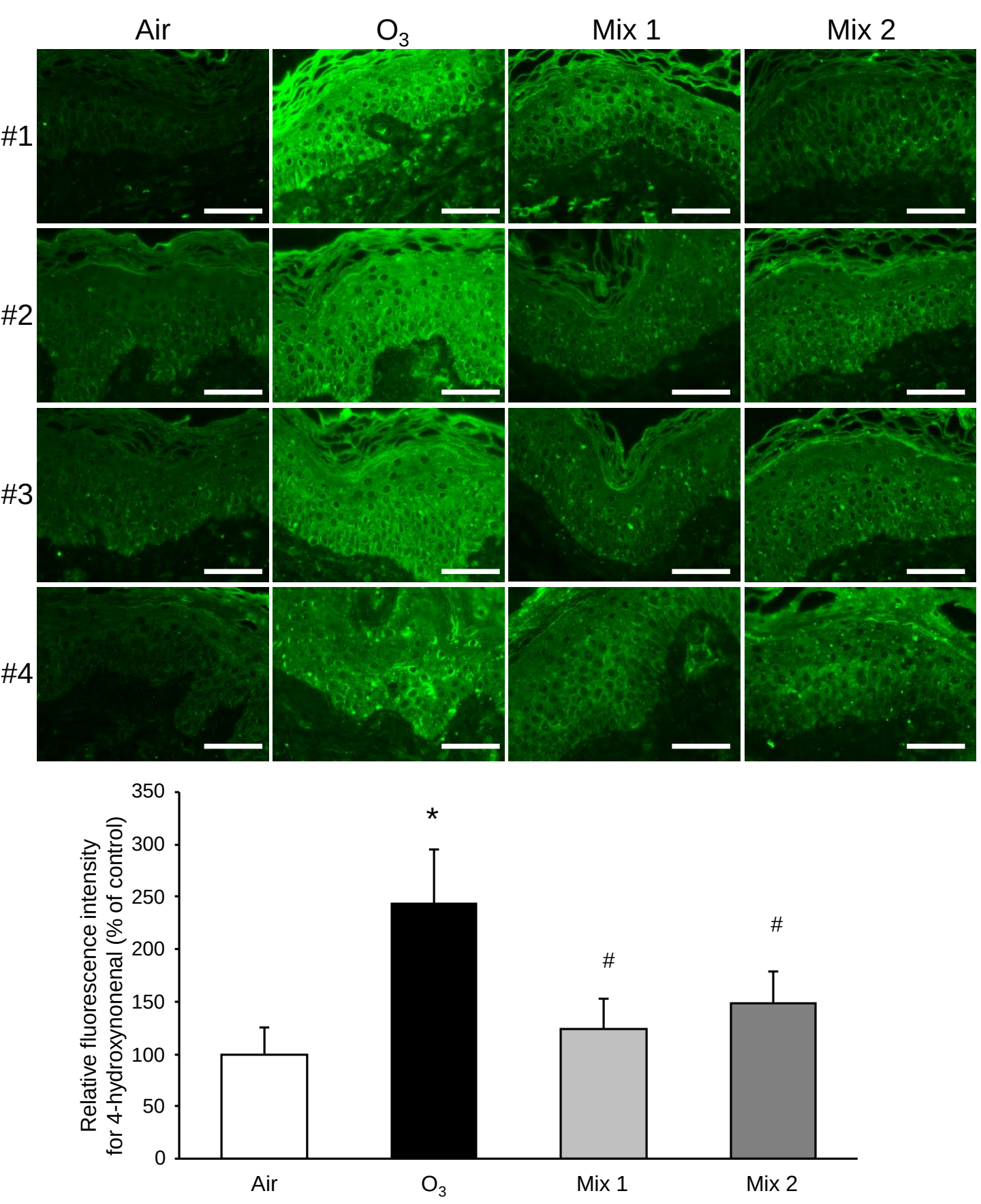

Supplementary Figure S1: Immunofluorescence for 4-hydroxynonenal in human cutaneous tissues treated with 2 different mixtures and then exposed to O_3. Representative images of human skin tissues (n=15) stained with 4HNE antibody. Original magnification x630. 4HNE signal (green fluorescence) was semi-quantified by using ImageJ software. Results are presented as means ± standard deviation. *P < 0.05 *vs* Air; $^{\#}P$ < 0.05 *vs* O_3.

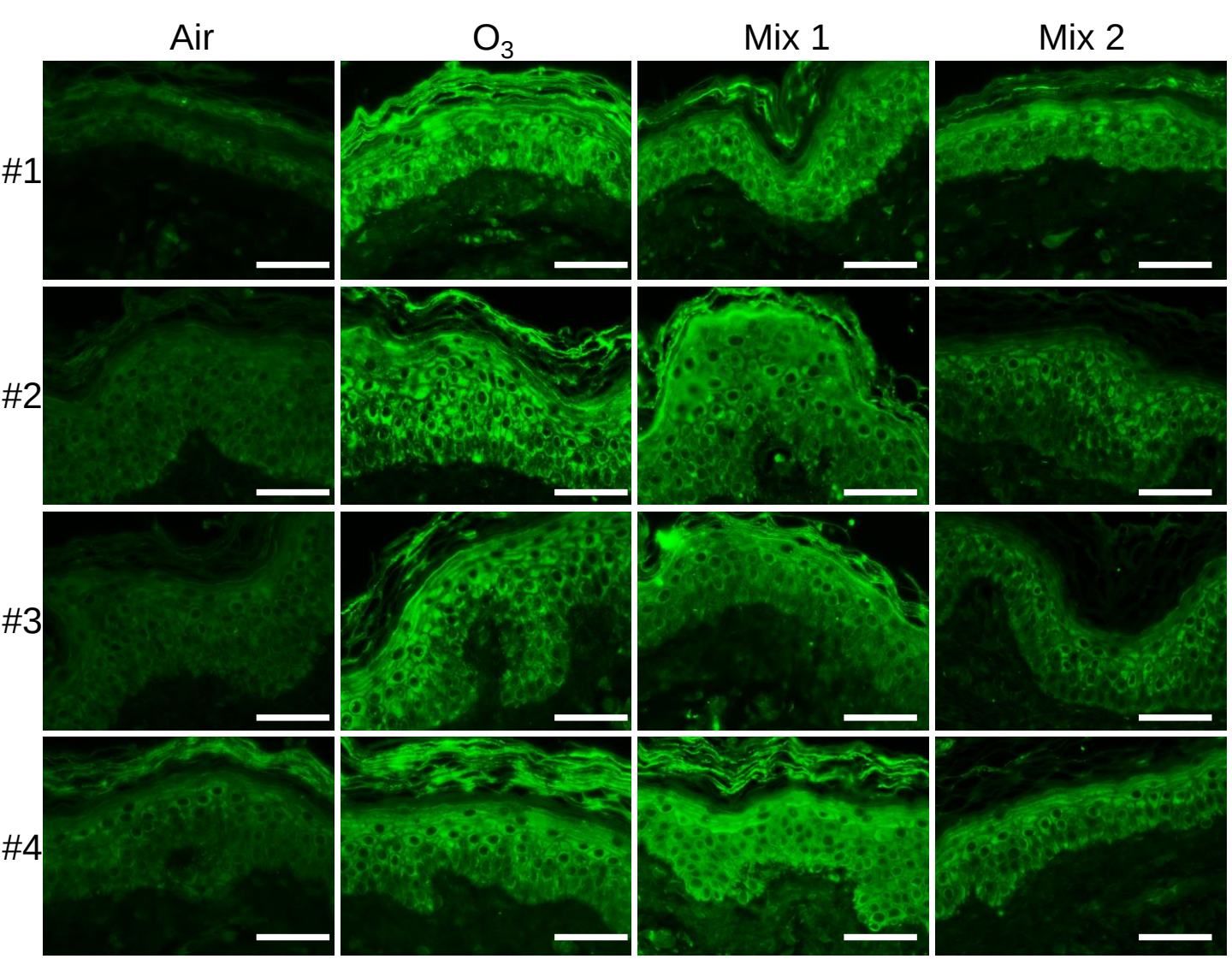

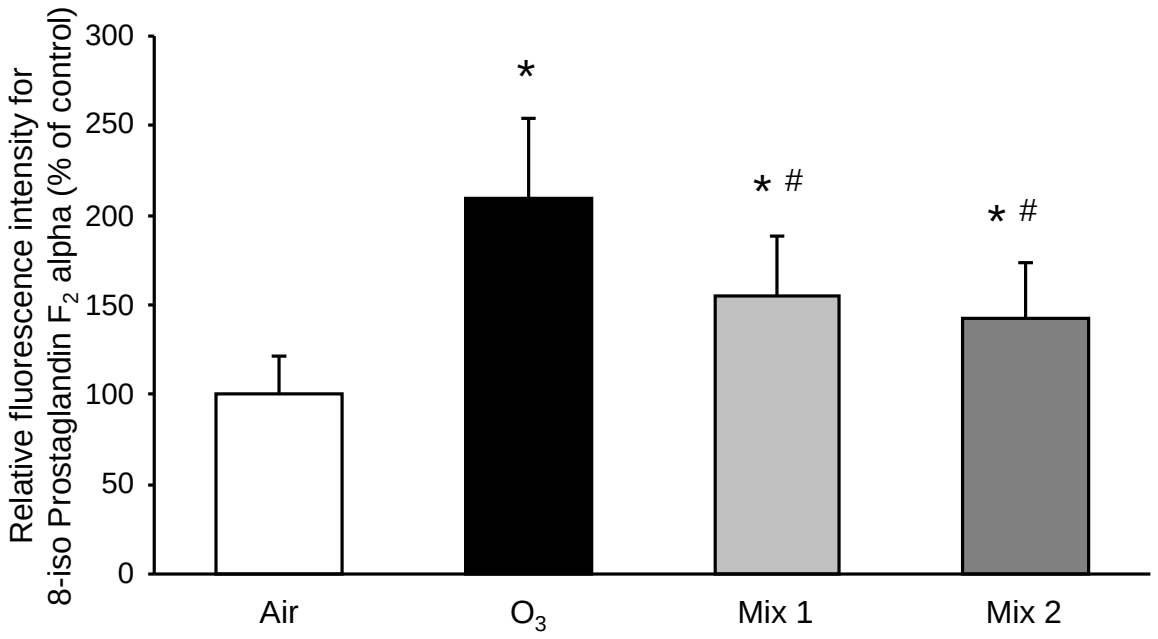

Supplementary Figure S2: Immunofluorescence for 8-iso Prostaglandin F_2 alpha in human cutaneous tissues treated with 2 different mixtures and then exposed to O_3. Representative images of human skin tissues (n=15) stained with 8-iso Prostaglandin F_2 alpha antibody. Original magnification x630. 8-iso Prostaglandin F_2 alpha signal (green fluorescence) was semi-quantified by using ImageJ software. Results are presented as means ± standard deviation. *$P < 0.05$ *vs* Air; #$P < 0.05$ *vs* O_3.

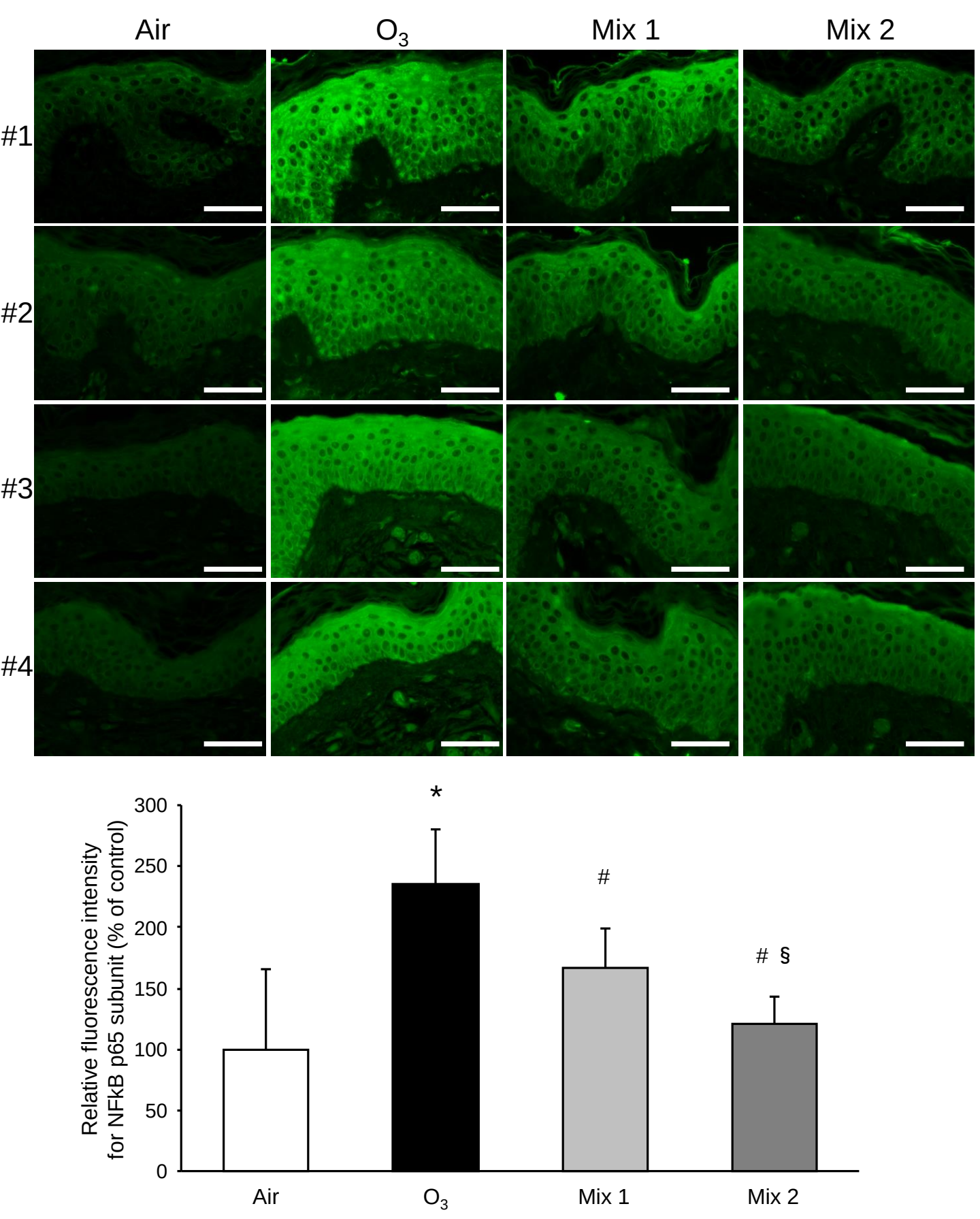

Supplementary Figure S3: Immunofluorescence for NF-κB p65 subunit in human cutaneous tissues treated with 2 different mixtures and then exposed to O_3. (a) Representative images of human skin tissues (n=15) stained with NF-κB p65 subunit antibody. Original magnification x630. (b) NF-κB p65 subunit signal (green fluorescence) was semi-quantified by using ImageJ software. Results are presented as means ± standard deviation. *$P < 0.05$ *vs* Air; $^{\#}P < 0.05$ *vs* O_3; $^{\S}P < 0.05$ *vs* MIX 1.

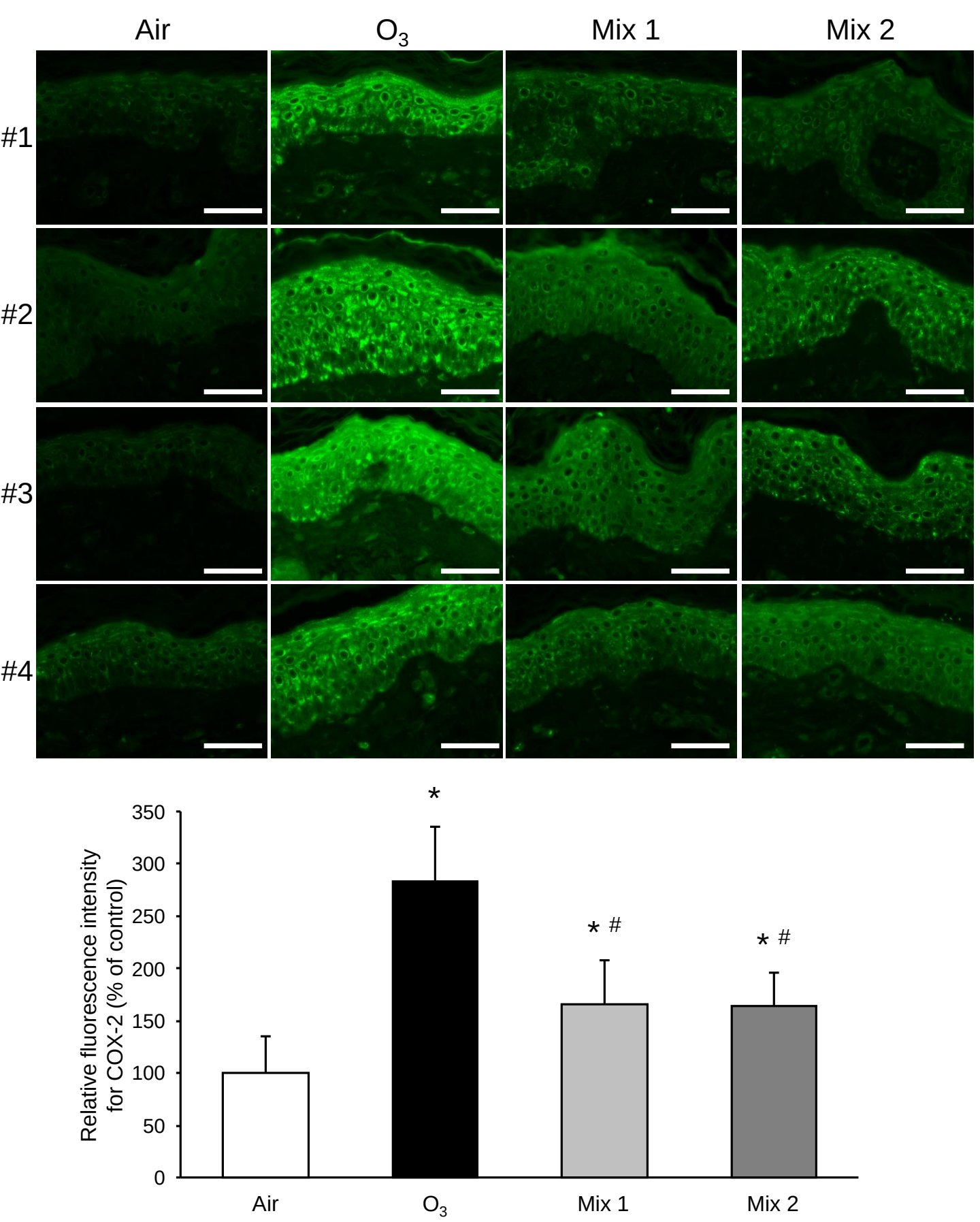

Supplementary Figure S4: Immunofluorescence for cyclooxygenase-2 in human cutaneous tissues treated with 2 different mixtures and exposed to O_3. (a) Representative images of human skin tissues (n=15) stained with COX-2 antibody. Original magnification x630. (b) COX-2 signal (green fluorescence) was semi-quantified by using ImageJ software. Results are presented as means ± standard deviation. *P < 0.05 *vs* Air; #P < 0.05 *vs* O_3.

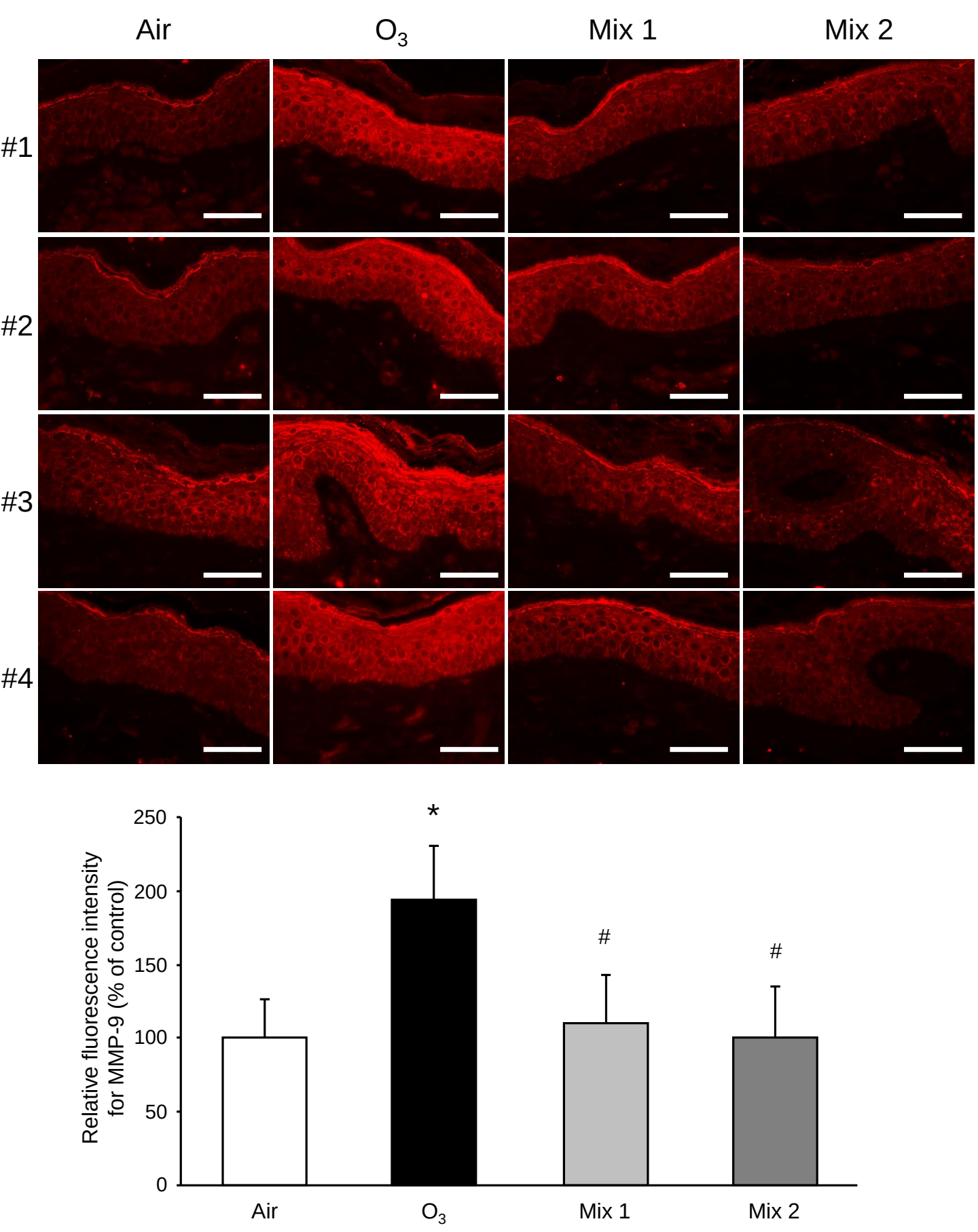

Supplementary Figure S5: Immunofluorescence for MMP-9 in human cutaneous tissues treated with 2 different mixtures and then exposed to O_3. (a) Representative images of human skin tissues (n=15) stained with an antibody specific to the active form of MMP-9. Original magnification x630. (b) COX-2 signal (red fluorescence) was semi-quantified by using ImageJ software. Results are presented as means ± standard deviation. $^{*}P < 0.05$ *vs* Air; $^{\#}P < 0.05$ *vs* O_3.

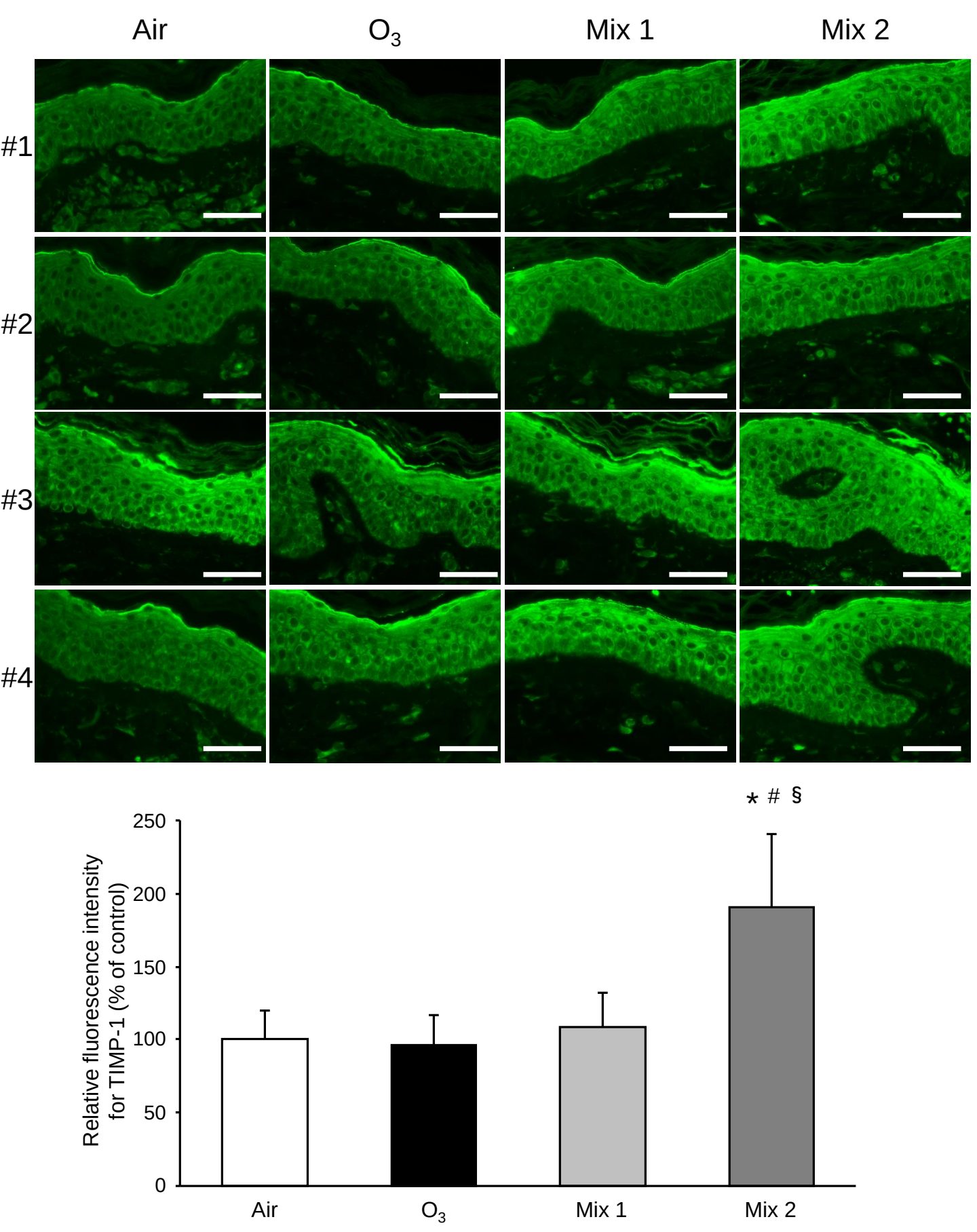

Supplementary Figure S6: Immunofluorescence for TIMP-1 in human cutaneous tissues treated with 2 different mixtures and then exposed to O_3. (a) Representative images of human skin tissues (n=15) stained with TIMP-1 antibody. Original magnification x630. (b) TIMP-1 signal (green fluorescence) was semi-quantified by using ImageJ software. Results are presented as means ± standard deviation. *P < 0.05 *vs* Air; #P < 0.05 *vs* O_3; § P < 0.05 *vs* MIX 1.

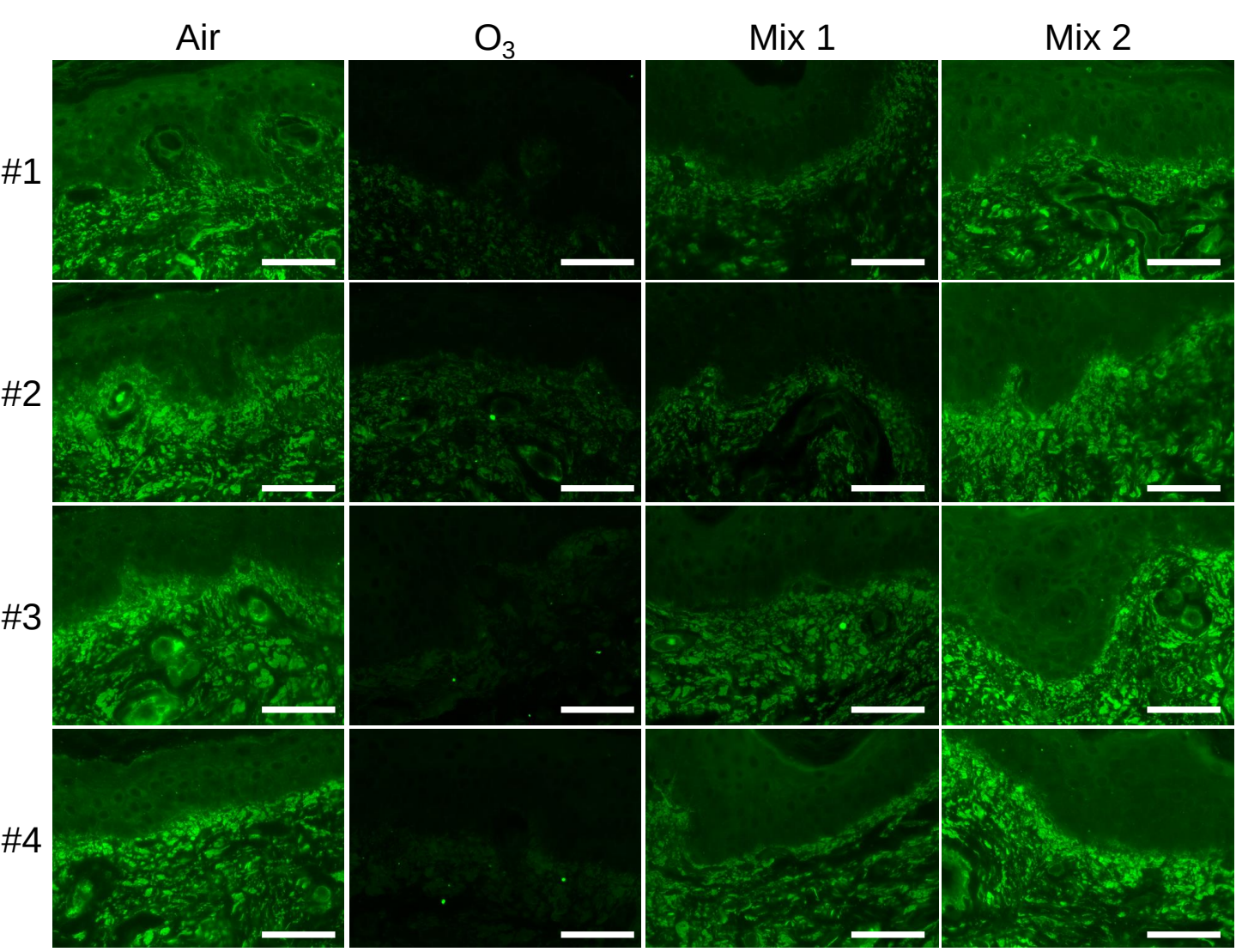

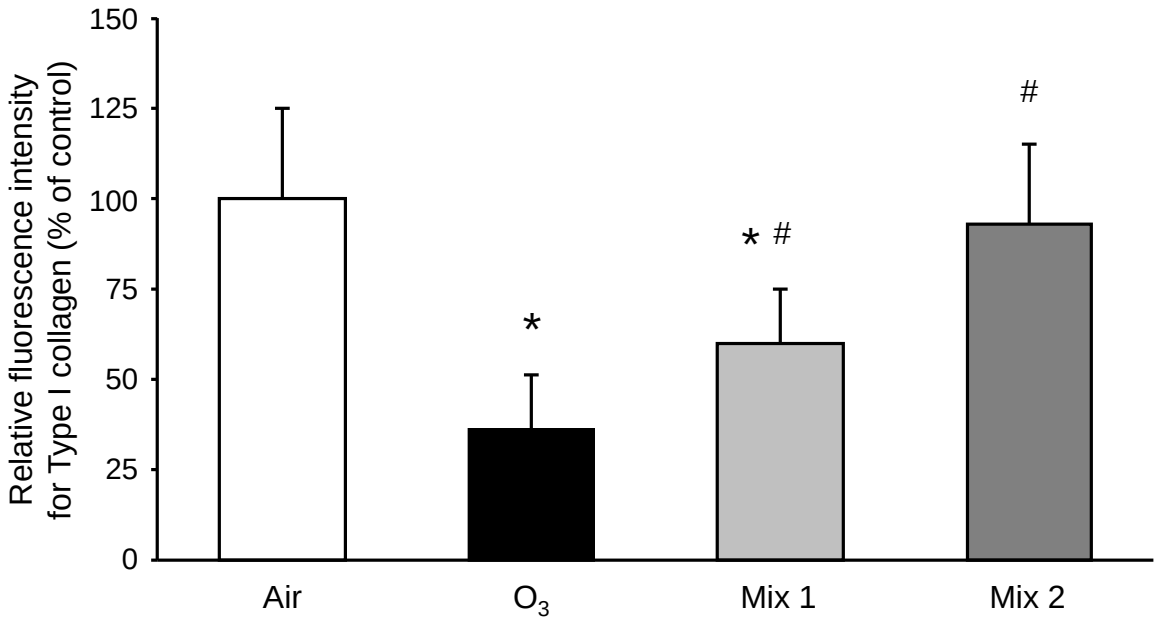

Supplementary Figure S7: Immunofluorescence for type I collagen in human cutaneous tissues treated with 2 different mixtures and then exposed to O_3. Representative images of human skin tissues (n=15) stained with type I collagen antibody. Original magnification x630. (b) Type I collagen signal (green fluorescence) was semi-quantified by using ImageJ software. Results are presented as means ± standard deviation. *$P < 0.05$ *vs* Air; #$P < 0.05$ *vs* O_3.

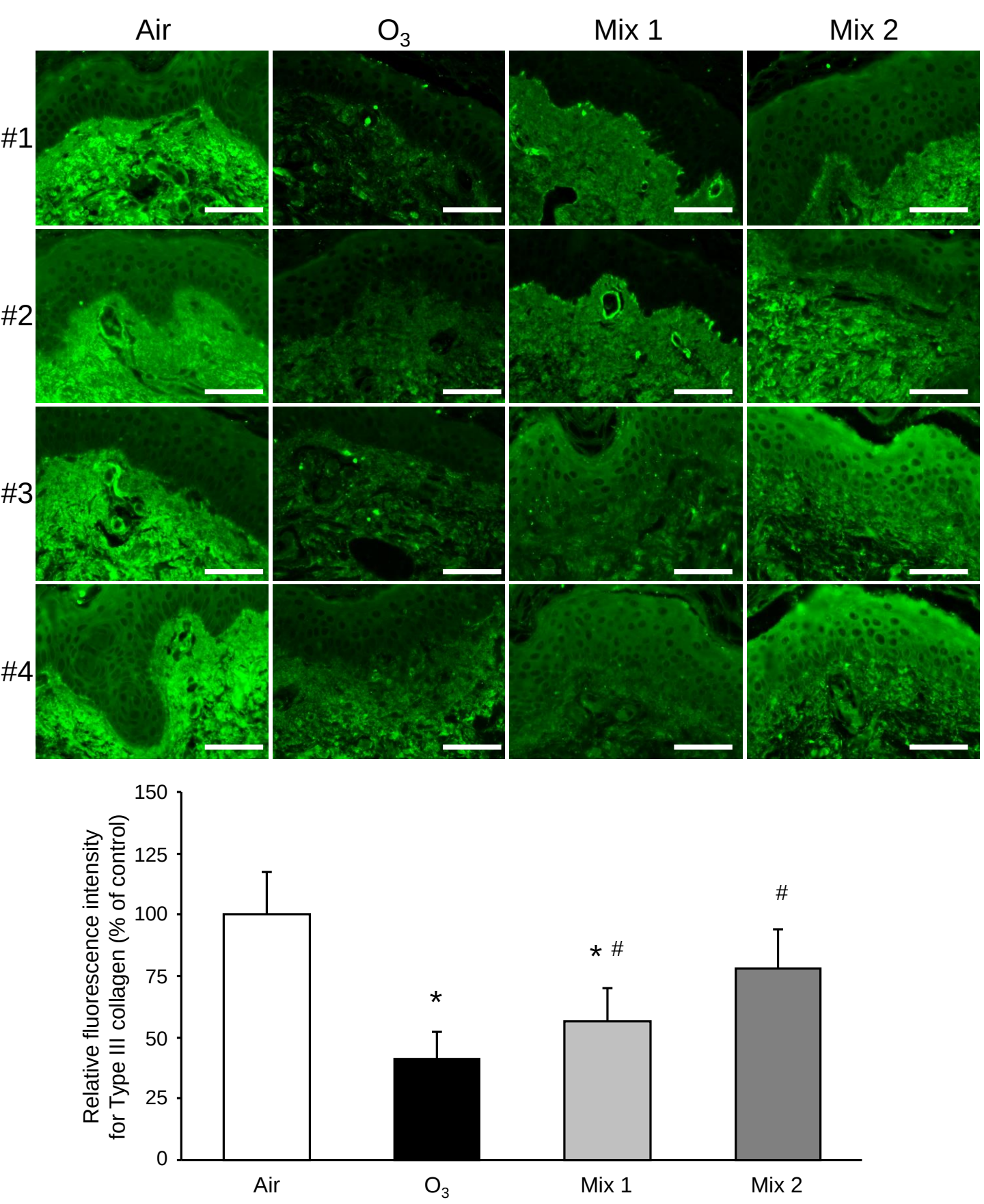

Supplementary Figure S8: Immunofluorescence for type III collagen in human cutaneous tissues treated with 2 different mixtures and then exposed to O_3. Representative images of human skin tissues (n=15) stained with type III collagen antibody. Original magnification x630. (b) Type III collagen signal (green fluorescence) was semi-quantified by using ImageJ software. Results are presented as means ± standard deviation. $^{*}P < 0.05$ *vs* Air; $^{\#}P < 0.05$ *vs* O_3.